Temperature dependence of dipolar modes in ferroelectric $BaTiO_3$ by infrared studies

J. A. Sanjurjo, R. S. Katiyar, and S. P. S. Porto*
Instituto de Física "Gleb Wataghin,"
Universidade Estadual de Campinas,
13100 - Campinas - S.P. - Brasil
(Received 4 February 1980)

Temperature dependence of A_1 modes in tetragonal phase and F_{1u} modes in cubic phase of $BaTiO_3$ has been studied by ir (infrared) reflectivity measurements. The spectra have been analyzed using Kramers-Kronig analysis and the coupled-mode classical oscillator fit. The results are in excellent agreement with each other and are compatible with the earlier Raman measurements. Such a compatibility indeed favors the conclusion of Pinczuk *et al.* with regard to the interpretation of the broad peaks at 270 and 520 cm^{-1} in the Raman spectrum to be of first order. A critical analysis of the earlier work in $BaTiO_3$ is presented.

I. INTRODUCTION

$BaTiO_3$ is one of the most important ferroelectric crystals in existence. As mentioned recently by Burns and Dacol[1]: "The structure phase instabilities and phase transitions of the perovskites, of which $BaTiO_3$ is the best example, was given a firm theoretical basis by the soft-mode theory of Cochran." This position of Burns and Dacol[1] is shared by a large number of physicists. Such conclusions, however, are not supported by recent studies on the Raman spectrum of $BaTiO_3$ by several workers.[2–6] These studies include the following: (a) The temperature dependence of Raman frequencies, linewidths, coupling parameters, and the dielectric behavior[2]; (b) experiments on polaritons and oblique polaritons for the A_1 (TO) modes, which could only be understood by a coupled-mode approach[3,4]; (c) a double-well disorder model for the crystal, which could explain quantitatively, the anomalous behavior of the linewidth of the ferroelectric mode of $BaTiO_3$ as well as the large change of the dielectric constant along the ferroelectric axis.[5,6] In order to complement these studies we have measured the infrared reflectivity due to A_1 modes at various temperatures and analyzed them by a 3-coupled-mode classical oscillator model. These results as well as the critical reading of earlier publications are presented in the following sections.

II. *E*-MODE STRUCTURE

To our knowledge the room-temperature *E*-mode spectrum of the tetragonal $BaTiO_3$ was completely understood in the work of DiDomenico *et al.*[7] based on the previous work by Pinczuk *et al.*[8] The spectrum is dominated by a strong overdamped mode with fitted frequency around 35 cm^{-1} which was indeed predicted by infrared reflectivity measurements.[9] Scalabrin *et al.*[2] studied the temperature dependence of the *E*-mode frequencies and the linewidths and accordingly, (a) there existed a large discrepancy between the measured value[10] of the dielectric constant in the *ab* plane and the one obtained from the Lyddane-Sachs-Teller relation. (b) The linewidth of the lowest overdamped *E*(TO) mode increased linearly with the temperature. These results were obtained using a damped harmonic oscillator fit to the spectra, but were independent of the fitting procedure contrary to what was suggested by Fleury and Lazay[11] and by Burns.[12] In a recent paper Burns and Dacol[1] have, however, confirmed the validity of the damped harmonic-oscillator fitting and obtained similar results to that of Scalabrin *et al.*[2] Another point to mention is that DiDomenico *et al.*[7] had reported a decrease in the intensity of the overdamped mode above 90 °C, which is in contradiction to the work of Burns and Dacol[1] and to that of Scalabrin *et al.*[2] This can be explained as due to the formation of multidomains above 90 °C in the crystal used by DiDomenico *et al.*[7]

III. A_1-MODE RAMAN SPECTRA

Much has been written and published on this subject. In 1967 Pinczuk *et al.*[8] identified all the (ZZ) Raman spectra as due to first-order scattering while DiDomenico *et al.*[7] identified the two broad bands at 270 and 520 cm^{-1} as second order for the following reasons: (a) The bands stayed practically unchanged through the phase transition at about 130 °C even though they are forbidden in the cubic phase; (b)

they were too broad and asymmetrical to be first order; (c) the 270-cm^{-1} band showed an odd line shape, later identified by Rousseau and Porto[13] as an interference with the low-frequency A_1 mode; (d) the two broad bands showed different frequencies and backgrounds in the (XX) and (ZZ) polarizations. Further work of Pinczuk *et al.*,[14] Benson and Mills,[15] Chaves *et al.*,[3,4] Scalabrin *et al.*,[2,16] and Verble *et al.*[17] confirmed the Pinczuk's original suggestion that all the features are of first order. Recently Burns and Dacol[1] returned to the subject and claimed that the two broad features at 270 and 520 cm^{-1}, which stay in the cubic phase, are not first-order bands and reaffirmed that all A_1 and E first-order spectra disappear at the Curie temperature as expected. Their argument is that in the region of 270 and 520 cm^{-1} there are two first-order bands superimposed on the second-order ones. Their interpretation, however, goes against published data of all the authors cited above, in particular, the work of Chaves *et al.*[3] form which Figs. 1(a), 1(b), and 1(c) are taken. These figures show the polariton spectrum of A_1 modes for various angles and also the calculated spectrum with a coupled phonon model approach. In the spectra at low angles it is shown that a band stays around 270 cm^{-1} but, as shown in the fit, this strength can be quantitatively explained as a phonon excited by the backscattered laser beam at the exit surface of the crystal. Burns and Dacol[1] have, however, overlooked this work and erroneously reported the conclusions drawn by the work of Pinczuk *et al.*[14] in which the authors stated that the two broad bands centered at 270 and 520 cm^{-1} correspond to TO phonons and their widths were explained by large anharmonic coupling and a frequency dependent damping constant. On the basis of the observed shifts in the frequency of the bands with the direction of the scattering wave vector relative to the c axis, Pinczuk *et al.*[14] concluded that the bands were first order. Moreover, in their work, Burns and Dacol[1] show the positions of the frequency of the two low A_1 modes by arrows, which appears to be an arbitrary choice. Further, their criticism of the coupled-mode calculations by Chaves *et al.*[4] and of Scalabrin *et al.*,[2] regarding the large coupling constant and the mode frequencies, away from the peaks in the spectra, can be explained as follows: in the case of coupled oscillators fitting using real coupling between the modes, the frequency parameters may not have physical meaning by itself; however, the "quasiharmonic" fre-

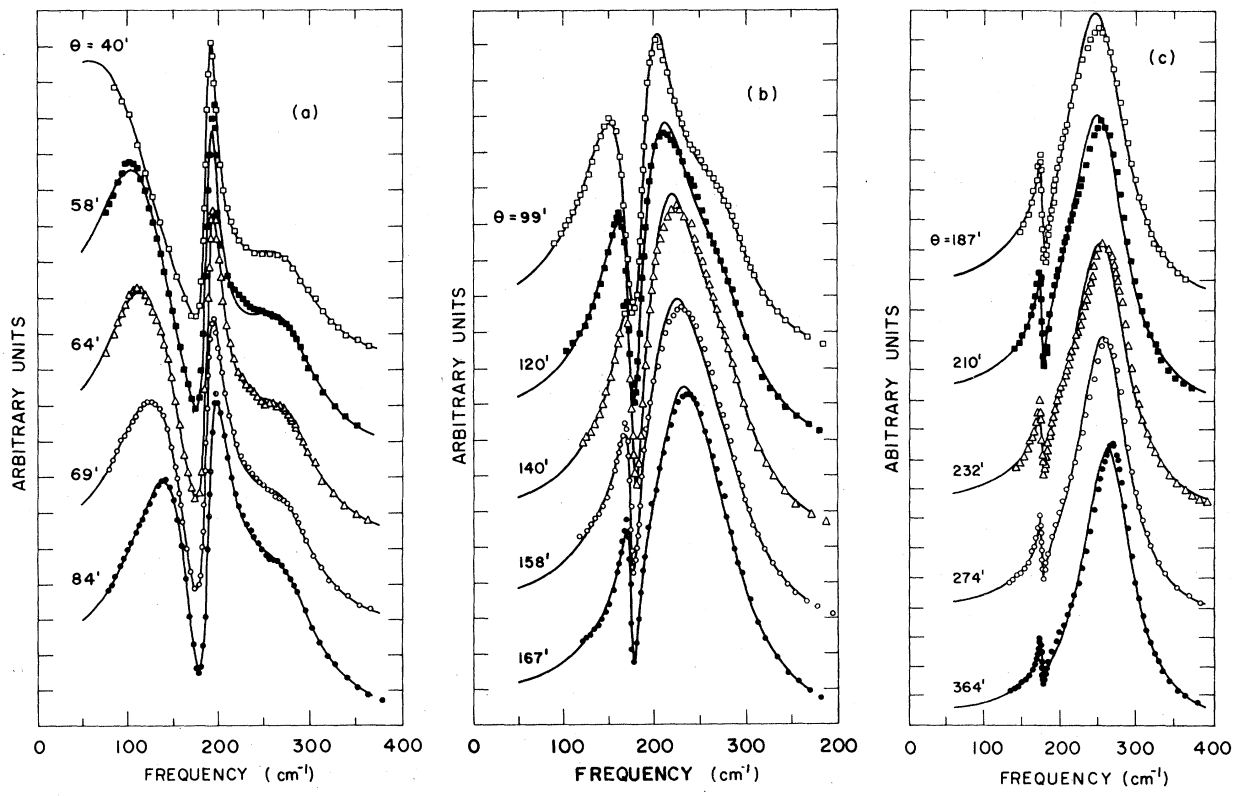

FIG. 1. (a)–(c) (ZZ) component of the two lowest polaritons of A_1 symmetry, the solid lines are the adjusted theoretical shapes with coupled-mode approach. The zero level of each curve is shifted two and one-half divisions in relation to its neighbors. The angles are internal ones and the resolution is 0.5 cm^{-1} for large angles and 1 cm^{-1} for small ones (Ref. 3).

quencies of these modes can be obtained either from the maxima of the imaginary part of the susceptibility function or by the diagonalization of the force matrix. This latter consideration has been discussed clearly in the case of two-mode coupling by Barker and Hopfield[18] and in the following part of this work. In order to settle the nature of the Raman spectra, it would be of great importance to obtain the A_1 infrared spectrum and compare it's results with the existing Raman data. We have carried out such studies and the results are presented in the following section.

IV. A_1-INFRARED REFLECTIVITY SPECTRUM

The experimental observation of the polarized infrared reflectivity with $\vec{E} \| \vec{c}$ (A_1 modes) was carried out on a large single-domain monocrystal in the region of 4000–50 cm^{-1} using the Perkin-Elmer-180 spectrophotometer equipped with a specular reflectivity accessory. The angle of incidence outside the crystal was within 15 degrees. The sample was put in an oven especially designed for the accessory and, using an Artronix temperature controller, the desired temperature was obtained within the variation of ± 0.5 °C. The polished face of the crystal containing a c axis was etched in order to remove the polishing effects from the surface in the manner described in an earlier paper.[19] The reflectivity spectra were analyzed using a coupled oscillator model as described below.

The possibility of phonon-phonon coupling via anharmonic interactions was first suggested by Barker and Hopfield[18] in order to improve the fitting of the E modes infrared reflectivity of $BaTiO_3$, as well as of $SrTiO_3$ and $KTaO_3$ (Spitzer's data[9]). Maradudin and Ipatova[20] pointed out that the existence of off-diagonal terms in the self-energy matrix results in the coupling of modes of the same symmetry.

This concept was applied successfully by Benson and Mills[15] to fit the two A_1 polaritons of $BaTiO_3$ using the large-angle data from Pinczuk *et al.*[14] and Burstein *et al.*[21] Moreover, the phonon-phonon coupling in Raman, Brillouin, and neutron scattering were observed in a large number of systems.[22–25]

Chaves *et al.*[4] extended the phenomenological approach of Barker and Hopfield[18] to an arbitrary number of modes and, considering a three-mode coupling, they obtained an excellent fit for A_1 phonons and polaritons.[3,4] They discussed the existence of unitary transformation that can diagonalize either the real part (imaginary coupling) or the imaginary part (real coupling) of the matrix response function. This latter case was first applied by Barker and Hopfield[18] in the case of two-mode coupling. However, Chaves *et al.*[4] and Katiyar *et al.*[25] have shown that this simple unitary transformation is not a general result and have found that the A_1 polariton shapes in $BaTiO_3$ and the B_2 phonon lineshape in KH_2AsO_4 (KDA), respectively, are best described by a pure real coupling between the modes. Later Scalabrin *et al.*[2] used the above approach to fit the right-angle A_1 (TO) Raman spectra as a function of temperature, obtaining reasonable results at all temperatures.

In order to fit the experimental reflectivity we use the following inverse matrix response function[2,4]

$$\vec{F}^{-1}(\omega) = -\omega^2 \vec{1} - i\omega \vec{\Gamma} + \vec{\Omega}^2 \quad , \tag{1}$$

where $\vec{1} = \{\delta_{ij}\}$ is the unit matrix, $\vec{\Omega}^2 = \{\omega_{ij}^2\}$ the force-constant matrix, and $\vec{\Gamma} = \{\gamma_{ij}\}$ the damping matrix.

At this point it is important to relate the phenomenological approach adopted here and the more general approach taken from the general dynamical theory of anharmonic crystals. To do this we follow the review paper of Whener and Steigmeier.[27] From the equation of motion of the phonon normal coordinates, the Dyson (matrix) equation for the retarded phonon Green's functions can be written as

$$G_{ik} = G_{ik}^{(d)} - \sum_{l \neq m} G_{il}^{(d)} \Pi_{lm}^{(nd)} G_{mk} \tag{2}$$

or equivalently for the inverse

$$\vec{G}^{-1} = \vec{G}^{(d)-1} + \vec{\Pi}^{(nd)} \quad , \tag{3}$$

where $\vec{\Pi}^{(nd)}$ is the off-diagonal part of the matrix self-energy and $\vec{G}^{(d)}$ is the solution of the Dyson equation containing only the diagonal part of the self-energy. That is

$$G_{ik}^{(d)} = G_i \delta_{ik} \quad , \tag{4}$$

where

$$G_i = \frac{2\omega_i}{(\omega_i^2 - \omega^2 - i\omega\gamma_i)} \quad . \tag{5}$$

Equation (1) corresponds to Eq. (2) with the following parametrization of the off-diagonal part of the self-energy

$$\Pi_{ik}^{(nd)}(\omega) = \Delta_{ik}(\omega) - i\Gamma_{ik}(\omega) \quad ,$$

with

$$\Delta_{ik}(\omega) = (4\omega_i\omega_k)^{-1/2}\omega_{ik}^2 \quad ,$$

$$\Gamma_{ik}(\omega) = \omega(4\omega_i\omega_k)^{-1/2}\gamma_{ik} \quad , \tag{6}$$

and

$$F_{ik}(\omega) = (4\omega_i\omega_k)^{-1/2} G_{ik}(\omega) \quad .$$

This model is a simplified form of linear coupling where Δ_{ik} corresponds to an elastic interaction "force" between the modes, and γ_{ik} accounts for a velocity-dependent dissipation of energy through the coupling mechanism, taking into account that the real and imaginary part of the self-energy are related by the

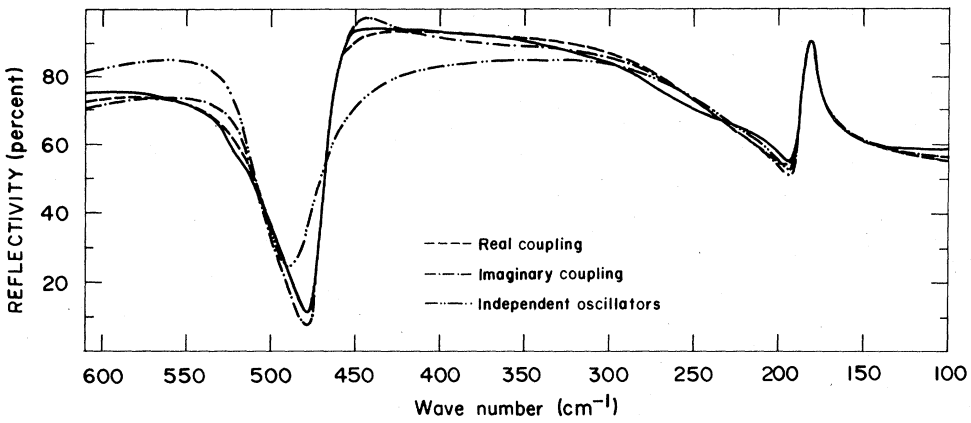

FIG. 2. Room-temperature ir reflectivity measurements parallel to the c axis (A_1 modes) shown by a solid line. The best fit with real coupling, imaginary coupling, and independent oscillator models are shown by dotted lines.

Kramers-Kronig relations.

For the complex dielectric function we use the following:

$$\epsilon(\omega) = \epsilon_{c,\infty} + \vec{Q}^{*+} \vec{F}(\omega) \vec{Q}^{*} \ , \tag{7}$$

where $\epsilon_{c,\infty}$ is the high-frequency dielectric constant parallel to the ferroelectric axis of the crystal, and $Q_i = Q_i^*/\omega_i$ are the oscillator charges for A_1 (TO) phonons.

The normal-incidence reflectivity is calculated from

$$R(\omega) = \left| \frac{\epsilon^{1/2}(\omega) - 1}{\epsilon^{1/2}(\omega) + 1} \right|^2 . \tag{8}$$

In Fig. 2 we show the experimental A_1 modes reflectivity at room temperature as well as the best fit with real coupling ($\Gamma_{ij} = \gamma_i \delta_{ij}$), imaginary coupling ($\Omega_{ij}^2 = \omega_i^2 \delta_{ij}$), and independent oscillators model ($\Omega_{ij}^2 = \omega_i^2 \delta_{ij}$, $\Gamma_{ij} = \gamma_i \delta_{ij}$).

In the coupled formalism we have not considered the interaction between the low- and high-frequency phonon, which is reasonable, because there is no spectrum overlap between them. It is obvious from the figure that the independent oscillator model failed to fit the measured reflectivity spectra. In Table I we have listed the resulting parameters of the fitting for each model and compared them with those obtained in previous works by Raman measurements.

The calculated imaginary part of the dielectric function for the three models is plotted in Fig. 3(a), where we indicated the peak positions in each case. The longitudinal frequencies of the modes were calculated from the zeros of the real part of the dielectric function plotted in Fig. 3(b). Their values are indicated by arrows. The computed transverse quasiharmonic and the longitudinal frequencies obtained from the fittings are listed in Table II. These values are in excellent agreement with the corresponding

TABLE I. Parameters associated with the zone-center A_1 (TO) phonons of tetragonal $BaTiO_3$ obtained from the best fit of the experimental data compared with previous Raman results. The parameters ω_i, ω_{ij}, γ_i, and γ_{ij} are measured in cm^{-1}, and Q_i are pure numbers.

Model	Q_1	γ_1	ω_1	ω_{12}	γ_{12}	Q_2	γ_2	ω_2	ω_{23}	γ_{23}	Q_3	γ_3	ω_3
Real coupling													
The authors	4.1	0.3	183	101	0	3.3	74	389	306	0	−0.95	7.6	423
Chaves *et al.*[a]	· · ·	2.0	179	82.7	0	· · ·	126.4	368	294	0	· · ·	5.5	463
Imag. coupling													
The authors	2.7	3.1	178	0	0.87	5.0	50	266	0	42	1.1	20	515
Chaves *et al.*[a]	· · ·	3.2	177	0	12.2	· · ·	89.7	283	0	54.5	· · ·	40.6	520
Independent oscillators													
This work	2.7	2.9	178	0	0	5.2	62.8	260	0	0	0.92	18.4	515
Pinczuk *et al.*[b]	2.78	· · ·	170	0	0	4.63	· · ·	270	0	0	1.00	· · ·	520

[a]Reference 4.

[b]Reference 14.

peaks in the Raman spectra,[2] except for the intermediate A_1 (TO) frequency, which is not as accurate because this mode appears as a smooth variation in the reflectivity spectra (see Fig. 2) as a consequence of the large coupling with the other two phonons and its large damping. There is a large uncertainty in the determination of the high A_1 (LO) phonon frequency because of the slowly varying real part of the dielectric function in the region of 700–750 cm^{-1}.

We have also carried out the Kramers-Kronig analysis for our experimental data and the imaginary part of the dielectric function thus obtained is shown in Fig. 4. As expected, the results are in good agreement with the classical oscillator fit. In Fig. 4, we

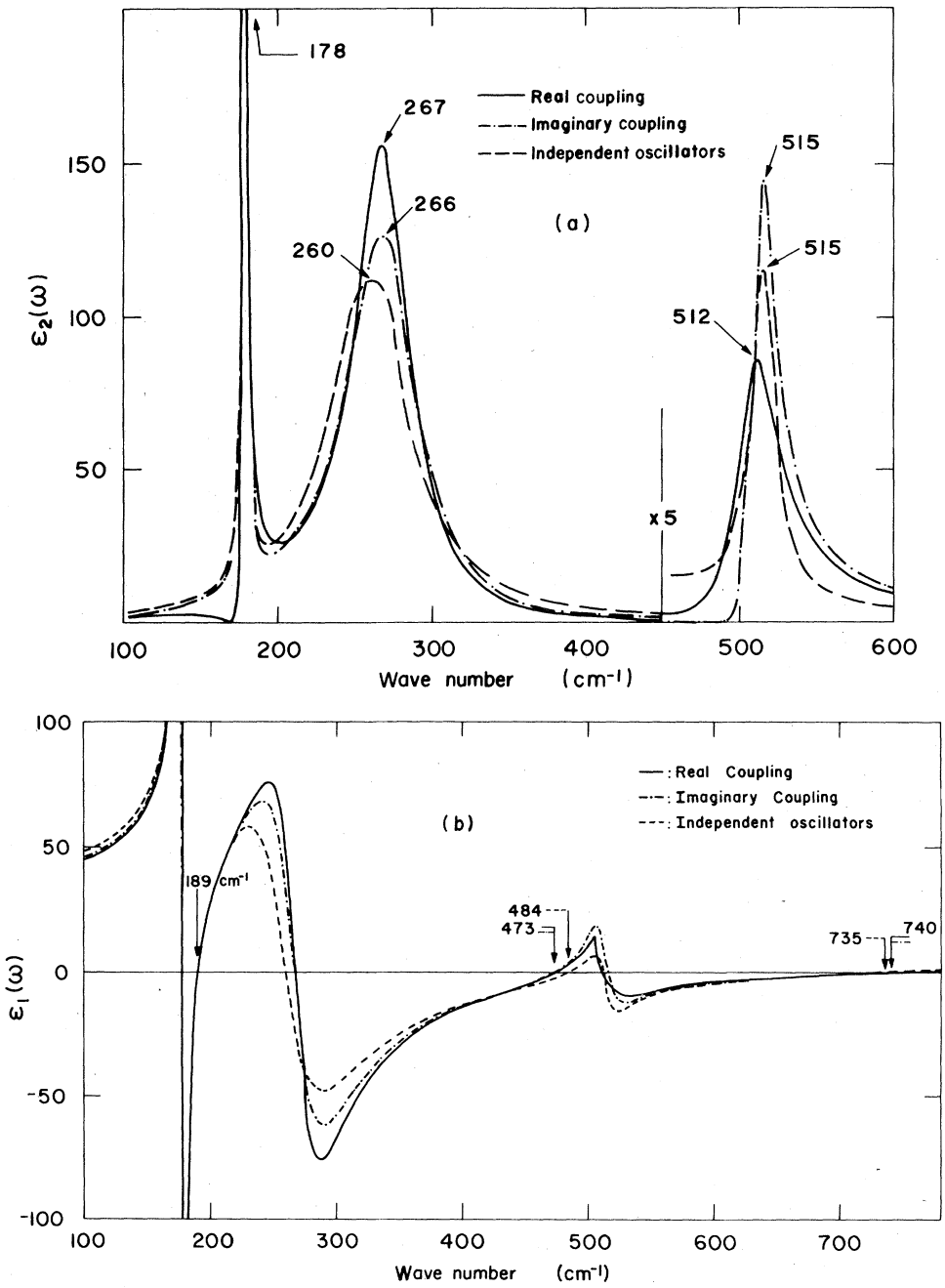

FIG. 3. Calculated imaginary part (a) and real (b) of the dielectric function from the best fit of ir reflectivity with real coupling, imaginary coupling, and independent oscillator models. The arrows indicate the positions of the "quasiharmonic" transverse and longitudinal frequencies of the modes.

TABLE II. Room-temperature A_1-modes quasiharmonic frequencies from the best fit of reflectivity with real coupling model and their comparison with Raman peaks.

Present ir work		Raman work[a]	
ω_{TO} (cm^{-1})	ω_{LO} (cm^{-1})	ω_{TO} (cm^{-1})	ω_{LO} (cm^{-1})
178	189	178	189
267	473	276	471
512	740	515	725
ϵ_0^c(LST) = 37		ϵ_0^c(LST) = 32	

[a]Reference 2.

have also shown the longitudinal modes obtained from the peak positions of the imaginary part of the inverse dielectric function.

The parameters obtained from the classical oscillator fit with real coupling were used to compute the A_1-modes Raman spectrum of $BaTiO_3$ at room temperature. To do this we use $I(\omega)$ for the Raman-Stokes response as given below:

$$I(\omega) = A(n+1)\,\mathrm{Im}\sum_{i,j}\beta_i\beta_j F_{ij}(\omega) \ ,$$

where A is a constant and β_i is the Raman oscillator strength. This spectrum compares well with the measured one, especially with regard to the peak positions and the region of interference. The results are plotted in Fig. 5.

The temperature variation of the reflectivity spectra are shown in Fig. 6. These spectra correspond to A_1 symmetry for temperatures below T_c ($T_c \cong 131\,^\circ$C) and to F_{1u} symmetry above T_c. A least-squares analysis using a coupled classical oscillator model was carried out for all of these spectra and the temperature variation of the quasiharmonic frequencies obtained from the best fit is shown in Fig. 7.

The lowest transverse-optic mode in the cubic phase is overdamped and because of the limitation in the lowest-frequency measurements to about 40 cm^{-1} in our spectrometer, we did not attempt to fit this F_{1u} mode and for computation we used the data from Ballantyne's work.[28] Our results compare well with those obtained by Burns.[29] It is, however, important to note that from the infrared reflectivity measurements shown in Fig. 6, the crystal of $BaTiO_3$ below the proper selection rules at the phase transition, i.e., the A_1 modes disapper at T_c and in the cubic phase only the F_{1u} modes are present. There are no extra peaks or features to be assigned as second order and the fact that the peaks and the line shapes in the Raman spectrum, with (ZZ) polarization at temperatures below T_c, coincide well with the first-order A_1

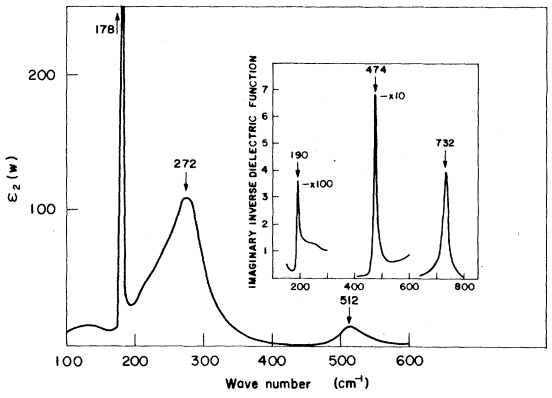

FIG. 4. Calculated imaginary part and imaginary inverse dielectric function from Kramers-Kronig analysis. The arrows indicate the positions of the "quasiharmonic" transverse and longitudinal frequencies of the modes.

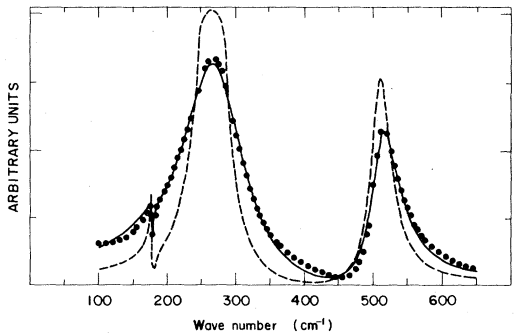

FIG. 5. Experimental $X(ZZ)Y$ A_1(TO) Raman spectrum at room temperature (solid line) and the calculated spectrum from the parameters of the best fit of reflectivity with real coupling model (dashed line). The dots are the best fit of the Raman spectrum with this model.

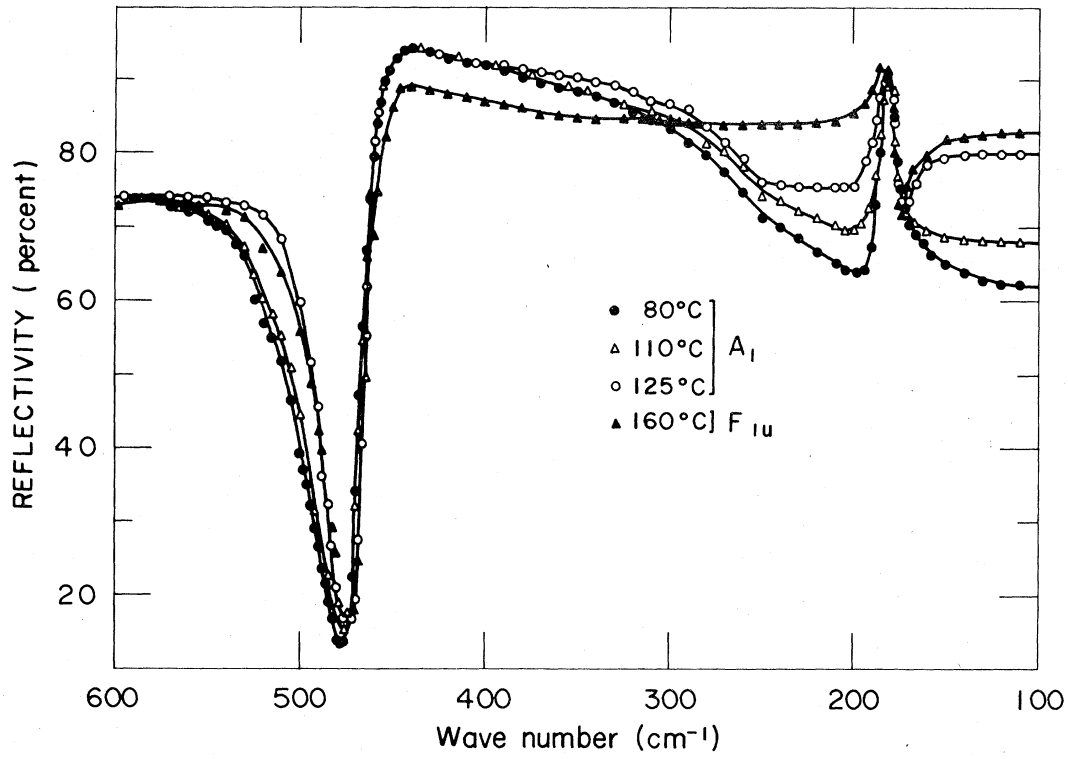

FIG. 6. Temperature behavior of the experimental ir reflectivity for A_1 modes (below T_c) and F_{1u} modes (above T_c).

modes obtained from the infrared measurements, allows one to identify the Raman spectrum of $BaTiO_3$ as first order. The extrapolated values of the dielectric constant parallel to the ferroelectric axis (ϵ_0^c) obtained from the infrared reflectivity fit [or from the Lyddane-Sachs-Teller (LST) calculation with the quasiharmonic frequency values] agree very well with those obtained from Raman measurements. However, it is very low, even at room temperature, compared with the capacitance measurements.

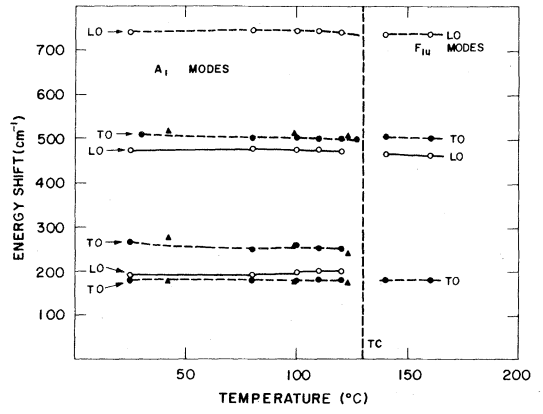

FIG. 7. Temperature variation of the "quasiharmonic" frequencies of A_1 and F_{1u} modes obtained from the best fit of ir reflectivity with real coupling model. The triangles are values obtained from Raman measurements taken from Ref. 29.

The question about the continued appearance of the two broad structures at about 270 and 520 cm^{-1} in the Raman spectrum of the cubic phase has been discussed by Fontana and Lambert.[30] From the temperature variation of the Raman cross section these authors conclude that the two broad bands cannot be a normal first-order effect, which is totally forbidden in a perfect perovskite structure, nor can it be an ordinary second-order scattering, since its intensities should increase quite rapidly with temperature. It is important to add that the "normal" second-order scattering in the perovskites, like $SrTiO_3$, is ordinarily very weak, but in the case of $BaTiO_3$ the two broad structures have almost the same intensities as in the tetragonal phase and they only appear with parallel polarization filters. All of these results, although not conclusive, seem to lend support to the order-disorder model proposed by Comes *et al.*[31] (CLG).

Recently progress has been made with the CLG model. Almeida[32] with a modified CLG model explains the differences that appear in the (XX) and (ZZ) polarization background of the A_1-modes Raman spectra in the tetragonal phase. Moreover, an eight-site order-disorder thermodynamical model was

applied by Oliveira *et al.*[33] to explain the differences between the phonon contribution and the capacitance measurements for directions parallel or perpendicular to the ferroelectric axis in the tetragonal phase. Further, a Hamiltonian in the spirit of the CLG disorder model, has been proposed recently by Silva *et al.*[34] and the thermodynamical functions are calculated for the three ferroelectric phases of $BaTiO_3$ in the mean-field approximation.

ACKNOWLEDGMENTS

The research support from FAPESP and CNPq is gratefully acknowledged.

---

*Deceased.
[1]G. Burns and F. H. Dacol, Phys. Rev. B 18, 5750 (1978).
[2]A. Scalabrin, A. S. Chaves, D. S. Shim, and S. P. S. Porto, Phys. Status Solidi B 79, 731 (1977).
[3]A. S. Chaves, P. R. Andrade, R. S. Katiyar, and S. P. S. Porto, in *Polaritons*, edited by E. Burstein and F. DeMartini (Pergamon, New York, 1974), p. 57.
[4]A. S. Chaves, R. S. Katiyar, and S. P. S. Porto, Phys. Rev. B 10, 3522 (1974).
[5]A. Scalabrin, S. P. S. Porto, H. Vargas, C. A. S. Lima, and L. C. M. Miranda, Solid State Commun. 24, 291 (1977).
[6]C. A. S. Lima, A. Scalabrin, L. C. M. Miranda, H. Vargas, and S. P. S. Porto, Phys. Status Solidi 86, 373 (1978).
[7]M. DiDomenico, S. H. Wemple, S. P. S. Porto, and R. P. Bauman, Phys. Rev. 174, 522 (1968).
[8]A. Pinczuk, W. T. Taylor, E. Burstein, and I. Lefkowitz, Solid State Commun. 5, 429 (1967).
[9]W. G. Spitzer, R. C. Miller, D. A. Kleinman, and L. E. Howarth, Phys. Rev. 126, 1710 (1962).
[10]S. H. Wemple, M. DiDomenico, Jr., and I. Camlibel, J. Phys. Chem. Solids 29, 1797 (1968).
[11]P. A. Fleury and P. D. Lazay, Phys. Rev. Lett. 26, 1331 (1971).
[12]G. Burns, Phys. Rev. B 10, 1951 (1974).
[13]D. L. Rousseau and S. P. S. Porto, Phys. Rev. Lett. 20, 1354 (1968).
[14]A. Pinczuk, E. Burstein, and S. Ushioda, Solid State Commun. 7, 139 (1969).
[15]H. J. Benson and D. L. Mills, Solid State Commun. 8, 1387 (1970).
[16]A. Scalabrin, S. P. S. Porto, and A. S. Chaves, in *Light Scattering in Solids*, edited by M. Balkanski, R. C. C. Leite, and S. P. S. Porto (Flamarion, Paris, 1976), p. 861.
[17]J. L. Verble, E. Gallego-Lluesma, and S. P. S. Porto, J. Raman. Spectrosc. 7, 7 (1978).
[18]A. S. Barker and J. J. Hopfield, Phys. Rev. 135, A1732 (1964).
[19]J. A. Sanjurjo, S. P. S. Porto, and E. Silberman, Solid State Commun. 30, 55 (1979).
[20]A. A. Maradudin and I. P. Ipatova, J. Math, Phys. 9, 525 (1968).
[21]E. Burstein, S. Ushioda, A. Pinczuk, and J. F. Scott, in *Light Scattering Spectra of Solids*, edited by G. B. Wright (Springer, New York, 1969).
[22]J. F. Scott, Phys. Rev. Lett. 21, 907 (1968).
[23]J. F. Scott, Phys. Rev. Lett. 24, 1107 (1970).
[24]A. Zawadovski and J. Ruvalds, Phys. Rev. Lett. 24, 111 (1970).
[25]R. S. Katiyar, J. F. Ryan, and J. F. Scott, Phys. Rev. B 4, 2635 (1971).
[26]A. S. Chaves, PhD. dissertation (University of Southern California, 1973) (unpublished).
[27]R. K. Whener and E. F. Steigmeier, RCA Rev. 36, 70 (1975).
[28]J. M. Ballantyne, Phys. Rev. 136, A429 (1964).
[29]G. Burns, Phys. Lett. A 43, 271 (1973).
[30]M. P. Fontana and M. Lambert, Solid State Commun. 10, 1 (1972); see also, A. M. Quittet and M. Lambert, Solid State Commun. 12, 1053 (1973).
[31]R. Comes, M. Lambert, and A. Guinier, J. Phys. Soc. Jpn. 28, 195 (1970); see also, M. Lambert and R. Comes, Solid State Commun. 7, 305 (1969).
[32]A. M. O. de Almeida, J. Phys. C 11, 4105 (1978).
[33]A. G. Oliveira, A. S. Chaves, and F. C. S. Barreto, Solid State Commun. 20, 743 (1976).
[34]N. P. Silva, A. S. Chaves, F. C. S. Barreto, and L. G. Ferreira, Phys. Rev. B 20, 1261 (1979).